CHAPTER 4

Wnt signaling induces maturation of Paneth cells in intestinal crypts.

Nature Cell Biology 7(4):381-386 (2005)

Wnt signaling induces maturation of Paneth cells in intestinal crypts.

Johan H. van Es [1, 5], Philippe Jay [2, 5], Alex Gregorieff [1, 5], Marielle E.van Gijn [1], Suzanne Jonkheer [1], Pantelis Hatzis [1], Andrea Thiele [1], Maaike van den Born [1], Harry Begthel [1], Thomas Brabletz [3], Mark M. Taketo [4] and Hans Clevers [1].

[1] Hubrecht Institute, Netherlands Institute for Developmental Biology, Uppsalalaan 8, 3584CT Utrecht, the Netherlands.

[2] Present address, Institut de Génétique Humaine (IGH), CNRS UPR 1142, 141, rue de la Cardonille, 34396 Montpellier cedex 5, France.

[3] University of Erlangen**,** Dept. of Pathology, Krankenhaustr. 8-10, 91054 Erlangen, Germany.

[4] Department of Pharmacology, Kyoto University Graduate School of Medicine, Yoshida-Konoé-cho, Sakyo-ku, Kyoto 606-8501, Japan.

[5] These authors made an equal contribution.

Abstract

Wnt signaling, transduced through β-catenin/Tcf4, maintains the undifferentiated state of intestinal crypt progenitor cells. Mutational activation of the pathway initiates the adenoma-carcinoma sequence. While all other differentiated epithelial cells migrate from the crypt onto the villus, Paneth cells home towards the source of Wnt signals, i.e. the crypt bottom. We find that expression of a Paneth gene program is critically dependent on Tcf4 in embryonic intestine. Moreover, conditional deletion of the Wnt receptor Frizzled-5 abrogates expression of these genes in Paneth cells in the adult intestine. Conversely, adenomas in APC mutant mice and colorectal cancers in man inappropriately express these Paneth cell genes. These observations imply that Wnt signals in the crypt can separately drive a stem-cell/progenitor gene program and a Paneth cell maturation program. In intestinal cancer, both gene programs are activated simultaneously.

Wnts induce Paneth cell maturation

Wnt signaling plays a key role in the intestinal epithelium (87). Central to this signaling pathway is the stabilization of β-catenin and its interaction with TCF transcription factors within the nucleus (39;40). Cytosolic levels of β-catenin are tightly regulated. In the absence of Wnt signals, a dedicated complex of proteins including APC, Axin and GSK3-β phosphorylates β-catenin, resulting in its ubiquitination and degradation by the proteasome (248;249). Signaling by Wnt factors inhibits the APC complex. As a result, β-catenin is stabilized and translocates into the nucleus where it interacts with nuclear Tcf transcription factors to drive the transcription of specific target genes (39;40). Mutational activation of the Wnt signaling pathway in intestinal epithelial cells inappropriately activates Tcf4 and initiates adenoma formation (10;11). We have recently determined the Tcf4 target gene program in colorectal cancer cells and have found that it is physiologically expressed in the proliferative crypt progenitors of the intestinal epithelium (69). As an integral part of this program, β-catenin and Tcf4 control expression of EphB cell sorting-receptors. These receptors allow the correct positioning of epithelial cells in a Wnt gradient along the crypt-villus axis (86).

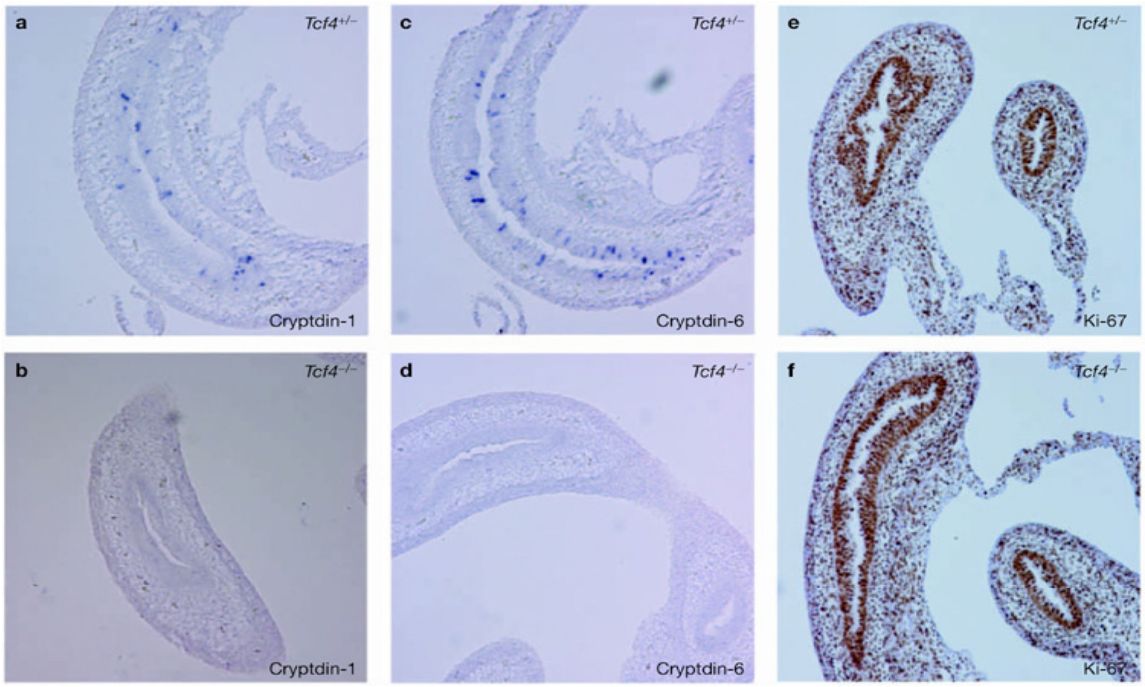

Figure 1. Cryptdins are target genes of the Tcf4-β-catenin signaling pathway.
Cryptdin-1 and Cryptdin-6 mRNA is readily detectable in the small intestine of $Tcf4^{+/-}$ E14.5 embryos (A, C), but is absent in $Tcf4^{-/-}$ embryos (B, D). No differences in proliferation were noted at E14.5 between $Tcf4^{+/-}$ and $Tcf4^{-/-}$ intestines as revealed by immunostaining for the proliferation marker Ki67 (E and F respectively).

Late embryonic mice deficient for the Tcf4 transcription factor fail to maintain the epithelial stem-cell compartments in the intervillus pockets of the small intestine (66). We utilized this genetic model to ask, by DNA array analysis, which genes are regulated by Tcf4 in the developing intestine. To this end, we compared expression profiles of $Tcf4^{-/-}$ and $Tcf4^{+/-}$ small intestines at E15.5, E16.5, and E18.5. As predicted, we identified multiple Tcf4 target genes (e.g. Myb, c-Myc, GPX-2, CDX-1) that were previously defined by inducibly blocking

the Wnt cascade in human colorectal cancer cell lines (69). Remarkably however, of the top-50 down-regulated genes, at least 8 encoded Paneth cell markers including several Cryptdins, Peptidoglycan Recognition Protein (PGRP) and Mpgc60 (see online version for Supplementary information, Table S1) (250-252). We realized that two previously published Tcf4 target genes in colorectal cancer cells, MMP7/Matrilysin (253) and EphB3 (86), also represent Paneth cell markers.

Paneth cells, which physically appear two weeks after birth, localize to the base of the crypts of Lieberkühn. They contain large apical secretory granules filled with a diverse array of antimicrobial proteins and peptides, including lysozyme and Cryptdins (254). The mouse Cryptdin gene family encodes at least 19 different Cryptdin proteins (255). In the small intestine, the Cryptdin-1 to -6 peptides are specific to Paneth cells (255). Cryptdin precursors are processed and activated in Paneth cells by the matrix metalloproteinase MMP-7 (256). Indeed, MMP-7-deficient mice do not process procryptdin precursors, resulting in a lack of mature Cryptdins and a defect in clearing intestinal infections (257). Below, we refer to the Tcf4-driven Paneth cell program as the MMP-7/Cryptdin program.

Despite the fact that Paneth cells are morphologically absent in embryonic and neonatal mice, the analyzed Cryptdin-1 and -6 mRNAs were readily detectable in the small intestine of $TCF4^{+/-}$ E14.5 embryos (Fig. 1A, 1C), yet absent from the small intestines of $Tcf4^{-/-}$ E14.5 embryos (Fig. 1B, 1D). Of note, the previously described $Tcf4^{-/-}$ phenotype, i.e. the abrogation of proliferation in the small intestinal epithelium, first becomes evident at E16.5 (66). Indeed, no differences were observed in expression of the cell cycle marker Ki67 at E14.5 (Fig. 1E, 1F).

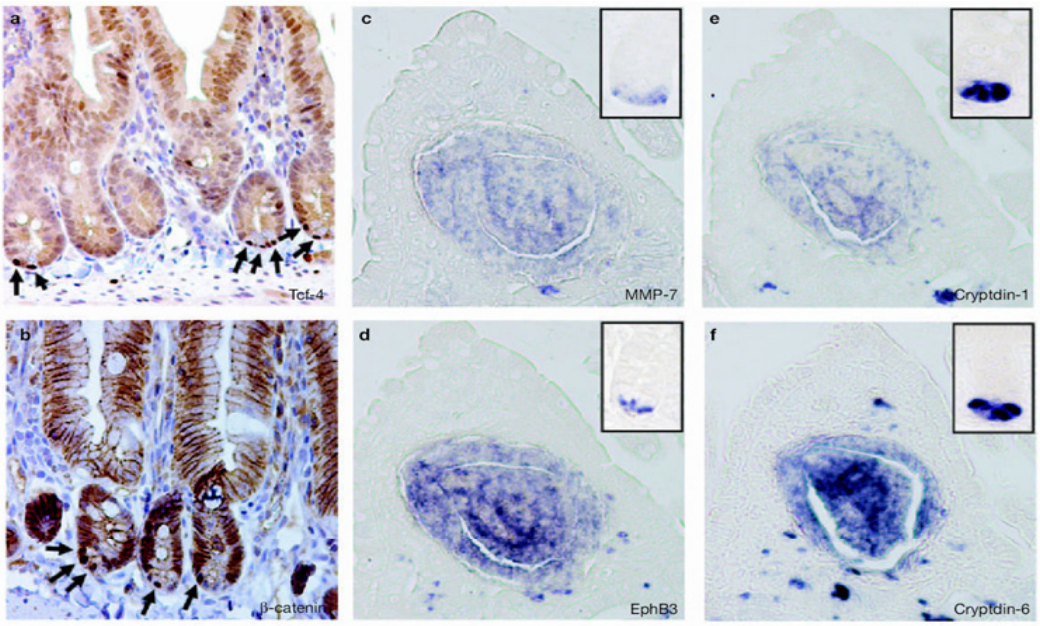

Figure 2. Strong nuclear expression of β-catenin and Tcf4 in Paneth cells and the upregulation of Paneth cell specific genes in APC^{min} tumors.
Immunohistochemical analysis revealed that the nuclei of Paneth cells contained high levels of the Wnt effectors Tcf4 (A) and β-catenin (B). *In situ* hybridization on the intestines of APC^{min} mice revealed that the Paneth cell genes MMP7 (C and (253)*)*, EphB3 (D and (86)) Cryptdin-1 (E) and Cryptdin-6 (F) are inappropriately expressed in adenomas. Inserts show normal Paneth cell expression of these Wnt targets in the intestinal crypt.

We have previously shown that proliferative crypt cells accumulate nuclear Tcf4 and β-catenin, indicative of active Wnt signaling. Similar analyses revealed that the nuclei of Paneth cells contained even higher levels of both Wnt effectors (Fig. 2A and 2B). Moreover, adenomas in APC mutant mice inappropriately expressed the MMP-7/Cryptdin program, including the genes encoding MMP7, EphB3, Cryptdin-1 and Cryptdin-6 (Fig 2C-2F). In addition, DNA array analysis on human colorectal cancers revealed that in the majority of these colon tumors (6 out of 8), the human functional counterparts of the Paneth cell-specific Cryptdins, Defensin-5 and Defensin-6 were also highly up-regulated (28.0 and 44.5 times, respectively).

The combined data suggested that the MMP-7/Cryptdin program contained direct Wnt target genes. We have previously determined a 12 bp optimal TCF binding site conserved from fly to man, AAGATCAAAGGG, where changes are tolerated in the first three bases only (258;259). Alignment of the promoters of murine Cryptdin-1, -2, -3, -5 and -6 revealed the complete conservation of a high-affinity TCF site, AAcATCAAAGGG (see Supplementary information Fig. S1). The promoters of human Defensin-5 and -6 also contain, at a conserved position, a high-affinity TCF-binding site fitting this consensus, AgcATCAAAGGG (see Supplementary information Fig. S1). A recent transgenic study has demonstrated that a 1402 bp promoter fragment of the human Defensin-5 gene faithfully drives Paneth-cell specific gene expression (260). A transient promoter assay demonstrated that this Defensin-5 promoter is indeed activated by β-catenin associated with endogenous Tcf through the conserved TCF site (Fig. 3A). The activation could be blocked by dominant-negative Tcf4 (Fig. 3A), while mutation of the conserved Tcf binding site in the Defensin-5 promoter also abrogated the activation by endogenous Tcf associated with β-catenin (Fig. 3B). Similarly, the murine Cryptdin-1 and Cryptdin-6 promoter were activated by the β-catenin/Tcf bipartite transactivation complex (Fig. 3C).

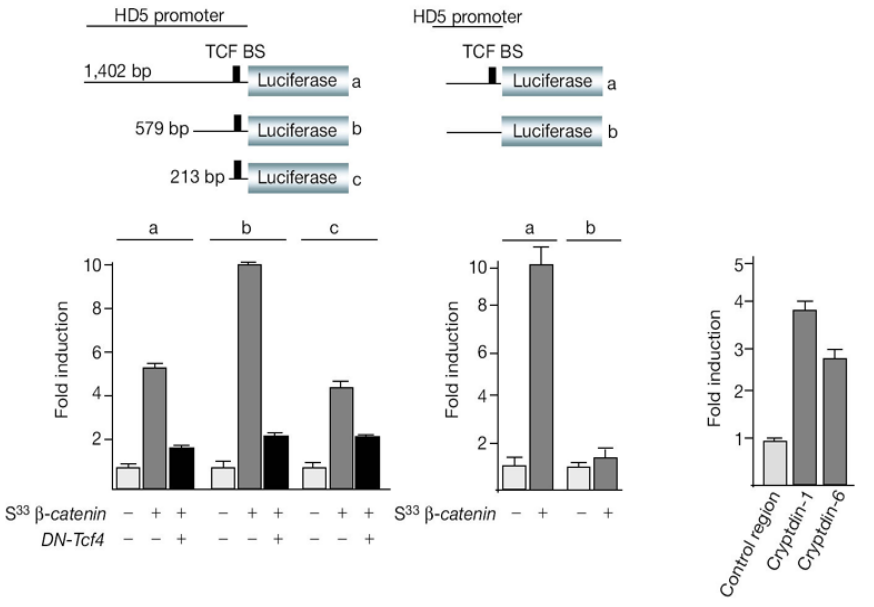

Figure 3. Tcf/β-catenin activation of the Cryptdin-1, Cryptdin-6 and Defensin-5 promoter through a highly conserved TCF binding site. Reporter construct containing deletions of the Paneth cell specific Defensin-5 promoter (260), containing a conserved TCF binding site (AAGATCAAAGGG) were generated. In a transient transfection assay, the Defensin-5 promoter constructs could be activated by an active Tcf/β-catenin bipartite transcription complex, which could be blocked by a dominant negative Tcf4 (A). The mutation of the highly conserved Tcf binding site (AAGATCCCCGGG) in the Defensin-5 promoter abrogated this Tcf/β-catenin

signaling (B). Reporter constructs of Defensin-5, Cryptdin-1 and Cryptdin-6 containing the highly conserved TCF binding site, could be activated by an active Tcf/β-catenin bipartite transcription complex (C). Chromatin immunoprecipitation analysis of the Cryptdin-1 and Cryptdin-6 promoters in Paneth-cell enriched crypt fractions revealed the occupancy of β-catenin. Bars represent Real-Time PCR values obtained with primers spanning the respective promoters normalized to the inputs and values obtained with primers spanning a control region downstream of the Cryptdin-6 gene, which was set to 1 for each calculation.

We also performed chromatin immunoprecipitations with an antibody directed against β-catenin on isolated mouse crypts (261). The results unambiguously demonstrated the presence of β-catenin on the promoters of Cryptdin-1 and -6 (Fig. 3), confirming the notion that these genes represent direct Wnt targets.

Independent of these experiments, we analyzed mRNA expression of all Frizzled family members in fetal and adult intestine by Northern blotting and *in situ* hybridization (A.G., submitted). In adult small intestine, we detected crypt-specific expression of 3 *Wnt* genes (*Wnt3*, and *Wnt9b*). Moreover, *Frizzled5 (Fz5)* and *Frizzled6* were prominently expressed in small intestinal epithelium. Interestingly, *Frizzled6* was expressed by all epithelial cells with the exception of Paneth cells, while Fz5 was expressed by all cells in the crypt. $Fz5^{-/-}$ embryos die *in utero* around E10 due to defects in yolk sac and placental angiogenesis (262). To analyze the function of *Fz5* in the adult intestine, we created a mutant *Fz5* allele, in which the single exon-open reading frame was sandwiched by LoxP sequences (see Supplementary information Fig. S2). We then generated germline chimeras and crossed their offspring with the intestine-specific K19-Cre knock-in mouse (263). The K19-Cre allele is expressed in a somewhat mosaic pattern throughout the intestinal epithelium from early stages of embryonic development into adult life (263). This was confirmed by the generation and subsequent analysis of a K19-LacZ knock-in mouse. This analysis revealed patchy expression of LacZ along the gastrointestinal tract (see Supplementary information Fig. S3). The expression of LacZ was highest in the duodenum and gradually declined along the gastrointestinal tract towards the rectum.

$Fz5^{LoxP/LoxP}$*K19-Cre* mice were healthy and fertile. Histological analyses of the entire gastrointestinal tract revealed a single abnormality. While the proliferative crypt compartment was intact, Paneth cells were randomly distributed in crypts and villi, as evidenced by morphology and by the markers lysozyme (Fig. 4D), FAS ligand (Fig 4E) and staining for Zinc-positive granules by the pholoxine tartrazine technique of Lendrum (Fig. 4E) (254;264;265). The highest number of miss-positioned Paneth cells occurred in the duodenum (not shown), coinciding with the expression of the Cre enzyme. The phenotype of miss-positioned Paneth cells was indistinguishable from that of $EphB3^{-/-}$ mice (86). Indeed, the miss-positioned Paneth cells of the $Fz5^{LoxP/LoxP}$*K19-Cre* mice never expressed the Tcf4 target gene *EphB3*, while the crypt Paneth cells did express EphB3 (Fig. 4G), providing an explanation for the observed miss-positioning and confirming our notion that the Wnt cascade provides positional clues along the crypt/villus axis (86). The miss-positioned Paneth cells appeared immature, based on the small size of their granules relative to those of Paneth cells in the crypts. These observations suggested that Fz5 plays a non-redundant role in the

transduction of canonical Wnt signals in the Paneth cell maturational process. Indeed, the miss-positioned Paneth cells displayed a complete absence of nuclear β-catenin (Fig. 4H). *In situ* hybridization revealed the absence of Cryptdin-1 mRNA in miss-positioned Paneth cells (Fig. 4L). Of note, the expression of the Tcf4-independent Paneth cell markers lysozyme remained unchanged, allowing for unambiguous identification of the Paneth cells (Fig. 4C, 4D, 4I, 4G and 4K resp.). In crypts of $Fz5^{LoxP/LoxP}$-*K19Cre* mice, some Paneth cells remained at the crypt base and expressed targets of the Wnt pathway. We reasoned that this resulted from the inefficiency of Cre-mediated deletion, due to the mosaic expression pattern of the Cre enzyme in these mice (263). Indeed, staining of the intestine derived from the $Fz5^{LoxP/LoxP}$-*K19Cre* mice revealed the presence of Fz5 expressing Paneth cells in the crypt, while all miss-positioned Paneth cells were Fz5-negative (Fig. 4F). In conclusion, the Wnt signaling pathway activates the MMP-7/Cryptdin maturation program in Paneth cells through the Fz5 receptor.

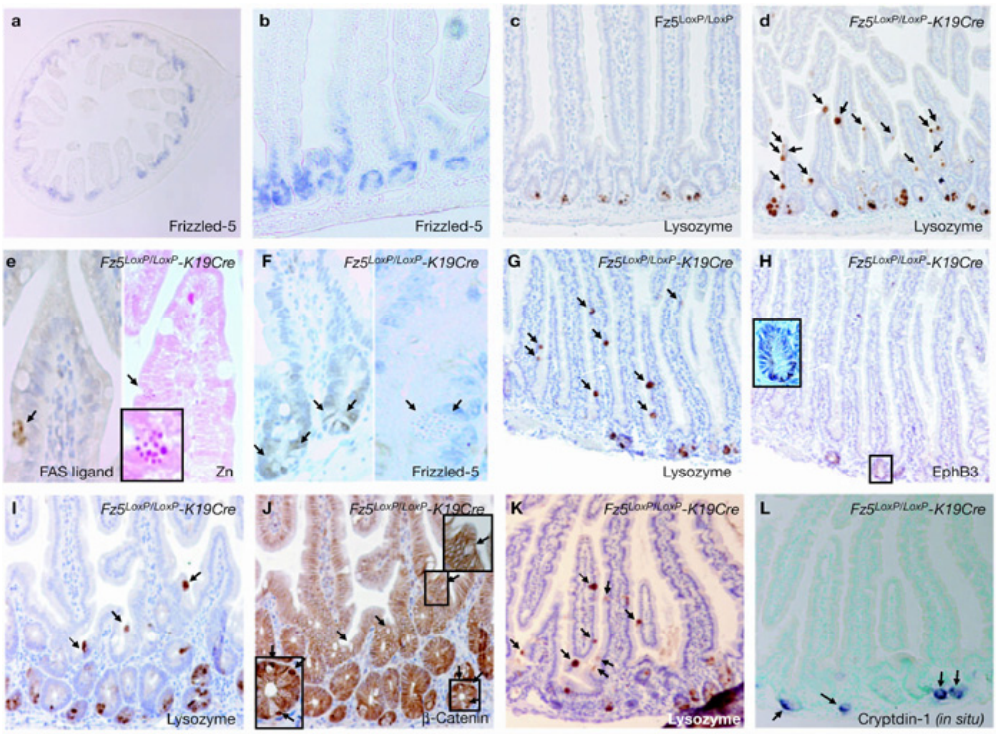

Figure 4. Paneth cells in the small intestine of $Fz5^{LoxP/LoxP}$ K19-Cre mice.
In situ hybridization with a Fz5 probe revealed that Fz5 is expressed in the (developing) crypts of neonatal (A) and adult mice (B). Staining of the intestine derived from $Fz5^{LoxP/LoxP}$ mice (C) and $Fz5^{LoxP/LoxP}$ K19-Cre mice (D-L). The panels G and H; I and J; and K and L represent three sets of serial sections. The panels C, D, G, I and K were stained with an antibody directed against lysozyme. Panel E were stained with an antibody directed against the FASligand and stained for Zn, Panel F with an antibody directed against Fz5, Panel H with an antibody directed against EphB3, Panel J with an antibody directed against β-catenin, and panel L with an *in situ* probe directed against Cryptdin-1. The Paneth cells of the $Fz5^{LoxP/LoxP}$ K19-Cre mice, in sharp contrast to the Paneth cells of $Fz5^{LoxP/LoxP}$ mice (C), stray from the crypt (B). Panel E shows that the mislocoalized Lysozyme positive cells also stained for the Fas ligand and contains Zinc-positivity of cytoplasmic granules. These markers unequivocally identify the mislocalized cells as Paneth cells. Panel shows that the mislocalized Paneth cells do not express Fz5, while the Paneth cells which stay at the bottom still express Fz5. The miss-positioned Paneth cells express the Paneth cell marker lysozyme (G, I, K), but lack expression of the Wnt signal transducer nuclear

β-catenin (J) or the Wnt target genes EphB3 (H), Cryptdin-1 (L) or Cryptdin-6 (results not shown). Insets in J show that the Paneth cells in the crypt do contain β-catenin in the nucleus (bottom left), whereas miss-positioned Paneth cells do not have nuclear β-catenin (top right).

The canonical Wnt signaling cascade is known to control multiple biological phenomena in vertebrates and model organisms, involving either cell fate determination or maintenance of stem/progenitor cells in compartments with predefined fates (64;174;266;267). A recent example of the latter is the role of Wnt signaling in the hematopoietic stem cell (268). The effect of Wnt signaling on Paneth cell maturation described here contrasts with this paradigm. In the absence of Wnt signals, Paneth cells are correctly specified, but fail to express the MMP-7/Cryptdin program. As a consequence, these postmitotic cells do not undergo morphological maturation. This adds a twist to the central role that the Wnt cascade plays in the biology of the crypt. Wnt signals near the bottom of crypts are crucial for the maintenance of the undifferentiated progenitors. Postmitotic immature Paneth cells, once specified, appear to utilize Wnt signals for the opposite aim: to reach full maturity through the Wnt-induced expression of the MMP-7/Cryptdin program.

Methods.

DNA array analysis.

DNA array analysis of mouse embryos. Total RNA was isolated from small intestine of $Tcf4^{+/-}$ and $Tcf4^{-/-}$ embryos (E15.5, E16.5 and E18.5) using TRIzol Reagent (Gibco BRL Life Technologies). cDNA synthesis and labeling were performed according to Affymetrix guidelines. Samples were hybridized on Murine Genome U74 arrays (Affymetrix) representing 36.000 full length genes and ESTs. Overall fluorescence for each GeneChip was scaled to a target intensity of 200 and pairwise comparisons were performed with Affymetrix MICROARRAY SUITE. Genes were selected based on the following criteria. For each time point, GeneChips for Tcf4 wt intestines were designated as baseline and all mRNAs which were decreased in $Tcf4^{-/-}$ intestines more than 1.5 fold in two out of three time points were selected.

DNA array analysis of human tumors. Detailed protocols and results will be published elsewhere (Hlubek et al., manuscript in preparation). In brief total RNA was separately prepared from eight microdissected human colorectal carcinomas and normal mucosa. Probe labelling and hybridisation to Affymetrix U133A arrays, representing 14,500 genes, were performed according to the Affymetrix guidelines (Affymetrix, Santa Clara, CA). The arrays include a set of human maintenance genes (> 100 probe sets) to facilitate the normalization and scaling of detected fluorescence values. This set of genes served as a tool to normalize expression levels, and allowed quantitative comparison of different tissues. Mean expression values of 8 tumours and normal colon mucosa were used to calculate the tumour/normal ratio of the selected genes.

Promoter analysis.

Schematic of the Defensin-5 deletion promoter constructs cloned in Pgl3basic (Promega). HEK293T cells were cotransfected with 500 ng of the indicated HD-5 promoter

constructs and/or plus 10 ng S^{33}β-catenin expression vector and/or 500 ng of a DN-Tcf4 expression vector and 50 ng of TK-Renilla reporter vector using Fugene (Roche). Total amounts of plasmid were kept constant by adding the empty DNA vector. The assays were harvested 20 hours later to assess luciferase and renilla activity using the dual-luciferase reporter assay (Promega). The assays were performed in triplicate and repeated at least three times. Data reported are normalized for transfection efficiency.

Chromatin Immunoprecipitation analysis on isolated crypts.

The Paneth-cell enriched crypt fractions were cross-linked with 1% formaldehyde for 10 min at room temperature, with gentle agitation. Cross-linking was terminated by the addition of glycine to a final concentration of 0.125M. The cells were washed twice with ice-cold PBS and swelled on ice for 10 min in 25 mM HEPES (pH 7.9), 1.5 mM MgCl2, 10 mM KCl, 0.5% NP40, 1 mM DTT and protease inhibitor cocktail (Roche). After Dounce homogenization the nuclei were resuspended in sonication buffer containing 50 mM HEPES (pH 7.9), 140 mM NaCl, 1 mM EDTA, 1% Triton X-100, 0.1% Na-deoxycholate, 0.5% SDS and protease inhibitors, sonicated for 4 min with 30 sec on and 2 min off cycles at high settings in a Diagenode Bioruptor to produce fragments with an average length of 400 bp. The chromatin was centrifuged, adjusted to 0.1% SDS, precleared and subjected to immunoprecipitation as described (261), with an antibody directed against β-catenin (BD Transduction Laboratories). The DNA in the immunoprecipitates was analyzed in SYBRGreen Real-Time PCR reactions on a MyiQ apparatus (Bio-Rad). The primers used for the PCR amplifications were the following: Cryptdin-1 promoter, sense: 5'-GGGAAATGGGAGTAGACTGAAG-3' and antisense: 5'-GGAAGTTGGAGAGGCTGTTAC-3', Cryptdin-6 promoter, sense: 5'-GATGGGAA ATGGGAGAAGACTG-3' and antisense: 5'-GGGAAGTTGGAAAGGGTGTTAC-3', control region downstream Cryptdin-6, sense: 5'-GCCATTCGGATGTTCACTCTG-3' and antisense: 5'- TCGTCTTGACCAACTGTTCT TG-3'.

Generation of the Cre inducible Fz5 KO mouse.

A P1 clone containing the mouse Fz5 gene was isolated from a mouse genomic library. The Fz5 coding region was PCR amplified (5'cgg gat cca gta ctg aat tcg ggc gtc aca ctc aag act cc3' and 5'cgc gga tcc aac agt aac ctc att aca atg cc3') and cloned between 2 LoxP sites of the modified pFlox vector. The 1 Kb 3'arm was subsequently cloned, followed by cloning of the 2.5 Kb 5' arm. Details of this construct are available on request. The construct was linearized and electroporated into E14 ES cells. Approximately 300 ES cell clones selected by neomycine (250 μg ml) were screened by Southern-blot analysis for the presence of a recombinant 2.4-kb *Eco*RI band, in addition to the endogenous 4.5-Kb fragment. A 350 bp PCR amplified fragment was used a probe (5'gat act agc acg tct gtc acc3' and 5'ccc cgc ggc ccc gcc cgg ag3'). Four out of 300 ES cell clones analyzed had undergone correct integrations at both ends of the construct. Chimaeric mice were derived from two randomly chosen clones; both transmitted the mutation through the germline.

Tissue sample preparation, immunohistochemistry and in situ hybridisation.

The intestinal tract was dissected as a whole and flushed gently with cold PBS to remove any faecal content. The small intestine was rolled up into a compact circle and fixed in Formalin at RT for 16 hours. The tissues were sectioned (2–6 μm). Following dewaxing and hydration, sections were pretreated with peroxidase blocking buffer (120 mM Na_2HPO_4, 43 mM citric acid, 30 mM NaN_3, 0.2% H_2O_2; pH 5.8) for 15 minutes at room temperature. Antigen retrieval was performed by boiling samples in Na-citrate buffer (10 mM, pH 6.0). After 20 minutes, the boiling pan was allowed to slowly cool down to room temperature. Incubation of antibodies was performed in BSA in PBS overnight at 4°C for antibodies directed against Cryptdin, Tcf4, Fz5 and MMP-7 and at RT for 1 hour for antibodies directed against lysozyme and Ki67. In all cases, the Envision$^+$ kit (DAKO) was used as a secondary reagent. The incubation time was 30 min. For goat antibodies, a bridge step using rabbit anti-goat antibodies was required. Stainings were developed using DAB. Slides were then counterstained with hematoxylin and mounted. The Fixation and staining of sections used for β-catenin and EphB3 expression was exactly as described (86). The following antibodies were used. Goat anti-EphB3 (1:100; R&D systems), Rabbit anti-lysozyme (1:1500; DAKO), Mouse anti-Ki67 (1:100; Novocastra), and mouse anti-β-catenin (1:50; Transduction Labs), Mouse anti-Tcf4 (1:400; Signal Transduction Lab), Goat anti-MMP-7 (1:50; R&D systems), Rabbit anti-Cryptdin-1 (1:1500; kind gift of Dr. Ouellette (269)), Rabbit anti-Frizzled5 (1:100; Upstate). *In situ* hybridizations were performed as described (270). As a probe for Cryptdin-1 and -6 we used anti-sense RNA derived from the Image clones 1096215 and 1545534 resp.

Wnts induce Paneth cell maturation